

## CASE REPORT

# Iliac access conduit facilitates endovascular aortic aneurysm repair and ipsilateral iliofemoral bypass

Hajime Kinoshita<sup>1</sup>, Eiki Fujimoto<sup>1</sup>, Hitoshi Sogabe<sup>2</sup>, Hiroshi Fujita<sup>2</sup>,  
Taisuke Nakayama<sup>1</sup>, Mikio Sugano<sup>1</sup>, Hirotsugu Kurobe<sup>1</sup>, Tamotsu Kanbara<sup>1</sup>,  
Takashi Kitaichi<sup>1</sup>, and Tetsuya Kitagawa<sup>1</sup>

<sup>1</sup>Department of Cardiovascular Surgery, Institute of Health Biosciences, the University of Tokushima Graduate School, Tokushima, Japan, <sup>2</sup>Imabari Daiichi Hospital, Ehime, Japan

**Abstract :** It may be difficult to access a route to deliver a stent-graft for abdominal aortic aneurysm in high-risk patients with bilateral iliofemoral occlusive disease. These two patients underwent both endovascular aortic aneurysm repair by a modified iliac access conduit technique and sequential ipsilateral iliofemoral artery bypass using the conduit, which provided excellent results. The iliac access conduit facilitates endovascular aortic aneurysm repair and ipsilateral iliofemoral bypass of high-risk patients with abdominal aortic aneurysm and bilateral iliofemoral occlusive disease. *J. Med. Invest.* 61 : 204-207, February, 2014

**Keywords :** *iliac access conduit, bilateral iliofemoral occlusive diseases, endovascular aortic aneurysm repair*

## INTRODUCTION

A combination of Trans-Atlantic Intersociety Consensus D iliofemoral occlusive disease and a significant abdominal aortic aneurysm (AAA) is occasionally encountered. Previous studies have shown that approximately 40%-70% of patients with AAA were anatomically unsuitable for endovascular aortic aneurysm repair (EVAR) due to bilateral iliofemoral occlusive diseases (1). Extensive calcified atherosclerotic disease, occlusions, and tortuous and/or narrow iliac arteries make the usual transfemoral access approach difficult. Two successful patients of both EVAR using the iliac access conduit as a safe endovascular arterial access and sequential iliofemoral artery bypass using the conduit are described in

this report.

### CASE 1.

A 77-year-old male exhibited both a huge infra-renal AAA and bilateral leg claudication. He had a history of cerebral infarction, hypertension and chronic kidney disease. Bilateral ankle-brachial pressure indexes (ABIs) were 0.75-0.80. Preoperative computed tomo-angiography revealed long complete occlusion of the right external iliac artery and severe stenosis of the left external iliac artery (Figure 1 (a)).

### CASE 2.

An 85-year-old male showed a significant infra-renal AAA and bilateral leg claudication. He had a history of chronic kidney disease and dementia. Preoperative bilateral ABIs were 0.71-0.72. Preoperative computed tomo-angiography revealed that the patient had complete occlusion of the left common iliac artery and severe stenosis of the right external iliac artery (Figure 1 (b)).

Received for publication August 1, 2013 ; accepted August 19, 2013.

Address correspondence and reprint requests to Hajime Kinoshita MD, Department of Cardiovascular Surgery, Institute of Health Biosciences, the University of Tokushima Graduate School 3-18-15 Kuramoto, Tokushima 770-8503, Japan and Fax : +81-88-633-7408.

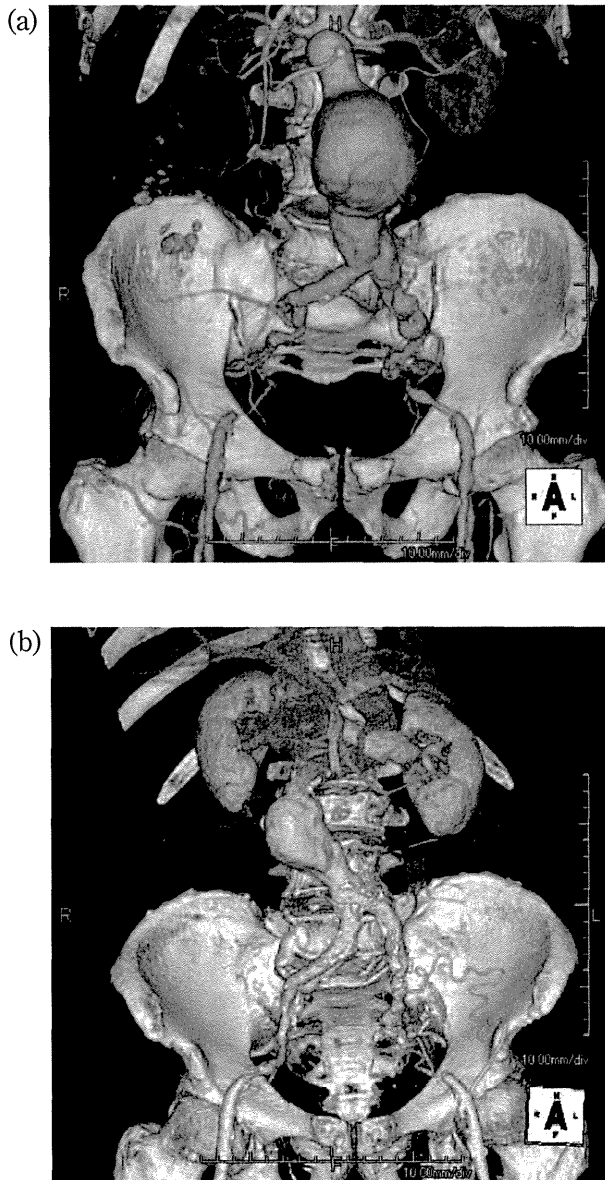


Figure 1. Preoperative 3D-computed tomo-angiography. Preoperative 3D-computed tomo-angiography showed complete occlusion of the right external iliac artery and severe stenosis of the left external iliac artery in Case 1 (a) and complete occlusion of the left external iliac artery and severe stenosis of the right external iliac artery in Case 2 (b).

The patients were of advanced age with poor activities of daily living, and they were high-risk patients for conventional open AAA repair and were unsuitable candidates with a poor access route for EVAR.

**SURGICAL TECHNIQUES**

1. The ipsilateral patent common iliac artery proximally placed to the long complete occlusion of the external iliac artery was exposed through a

retroperitoneal approach. Simultaneously, bilateral common femoral arteries were exposed by inguinal incision.

2. Percutaneous transluminal angioplasty (PTA) with stent placement was performed for short occlusion and/or stenosis of the contralateral external iliac artery antegradely and/or retrogradely.
3. An 8-mm Dacron graft was anastomosed in an end-to-side fashion to the ipsilateral distal common iliac artery as a safe iliac access conduit for EVAR (Figure 2 (a)).
4. After completion of the anastomosis, the delivery sheath (18-Fr introducer) of EVAR was inserted to the proximal site of the iliac conduit through a purse-string suture of the distal side aspect of the Dacron graft itself to avoid excess bleeding under fluoroscopic guidance.

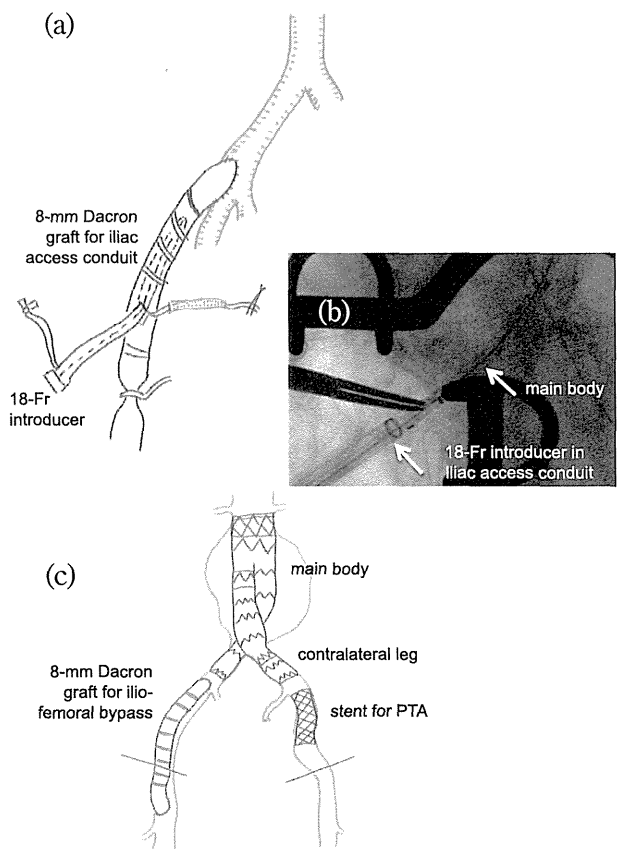


Figure 2. Operative schema and intraoperative fluoroscopic image for endovascular repair in Case 1. An 8-mm Dacron graft was anastomosed in an end-to-side fashion to the right distal common iliac artery as a safe iliac access conduit for endovascular aortic aneurysm repair (a). Main body of stent-graft was inserted through a delivery sheath (18-Fr introducer) at the distal side aspect of the iliac access conduit under intraoperative fluoroscopic guidance (b). Completion of endovascular aortic aneurysm repair, PTA and iliofemoral bypass was shown (c). Fr= French, PTA=percutaneous transluminal angioplasty

5. The main body of Y-type stent-graft was inserted through the delivery sheath and deployed from below the inferior renal artery orifice to proximal site of the common iliac artery-conduit anastomosis (Figure 2 (b)).
6. An additional stent-graft for the contralateral leg was delivered in the contralateral common iliac artery through the external iliac artery immediately reconstructed in advance by PTA.
7. After completion of EVAR, the iliac access conduit was used for ipsilateral iliofemoral bypass graft under the inguinal ligament (Figure 2 (c)).

## POSTOPERATIVE COURSES

Perioperative blood loss was well limited. Both postoperative courses were uneventful. There were no significant complications associated with EVAR, PTA and an iliofemoral bypass. Follow-up is complete in both patients and they are free from aggravation of heart and renal failure after operation. To date, both conduits remain patent, and both patients are alive and doing well with improved activities of daily living.

## DISCUSSION

An iliac access conduit for endovascular access was first reported as “perspective” and “access problems” by Parodi *et al.* (2). They reported that an aorto-uni-iliac stent-graft combined with the extraanatomical femorofemoral bypass is useful for AAA with diseased ilio-femoral arteries. Subsequently, EVAR using the iliac access conduit and ipsilateral ilio-femoral bypass through a retroperitoneal approach was first reported by Yano *et al.* in 2001 (3) and by Lee WA *et al.* in 2002 (4). We modified this technique together with PTA for contralateral iliac arterial disease.

The techniques of EVAR using the iliac access conduit concomitant with PTA of contralateral iliac artery disease and ipsilateral iliofemoral bypass using the iliac access conduit were superior in terms of not only completion of an anatomical vascular reconstruction in patients with bilateral iliac artery occlusive diseases but also not putting the thick delivery sheath of the main body of EVAR through the native narrow and tortuous diseased iliac arteries, which potentially decreases the risk of access route injuries (Figure 3).

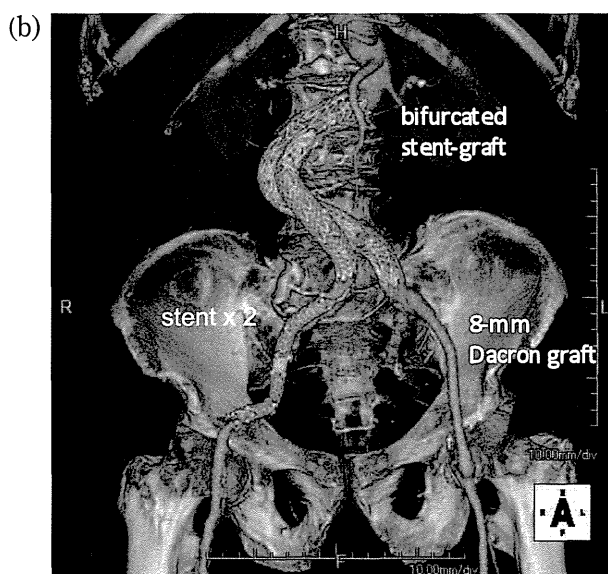
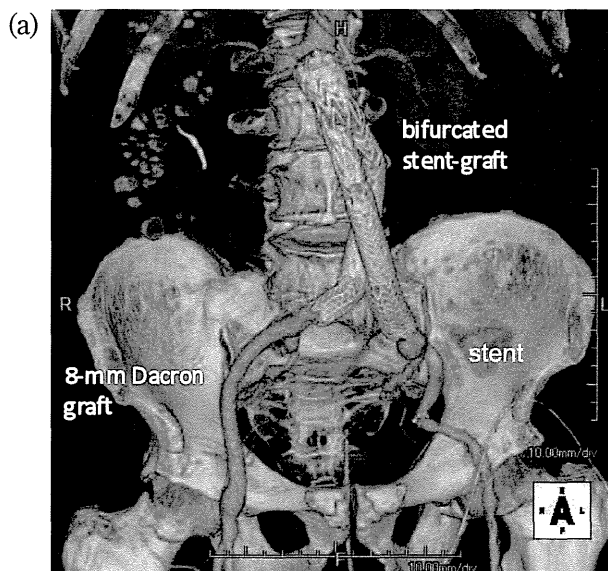


Figure 3. Postoperative 3D-computed tomo-angiography. Postoperative 3D-computed tomo-angiography showed successful completion of an anatomical vascular reconstruction in Case 1 (a) and in Case 2 (b).

We performed EVAR using an 18-French introducer not from the terminal end of the iliac access conduit but from the side aspect of the iliac access conduit. This contributed greatly to reduction of bleeding during passage of the delivery sheath (5).

We believe that the use of such techniques will ultimately increase the number of patients eligible for EVAR and avoid devastating access-related complications.

## CONFLICT OF INTEREST

We have no conflict of interests to disclose.

## REFERENCES

1. Woodburn KR, Chant H, Davies JN, Blanshard KS, Travis SJ : Suitability for endovascular aneurysm repair in an unselected population. *Br J Surg* 88 : 77-81, 2001
2. Parodi JC, Barone A, Piraino R, Schonholz C : Endovascular treatment of abdominal aortic aneurysms. *J Endovasc Surg* 4 : 102-110, 1997
3. Yano OJ, Faries PL, Morrissey N, Teodorescu V, Hollier LH, Marin ML : Ancillary techniques to facilitate endovascular repair of aortic aneurysms. *J Vasc surg* 34 : 69-75, 2001
4. Lee WA, Berceci SA, Huber TS, Seeger JM : A technique for combined hypogastric artery bypass and endovascular repair of complex aortoiliac aneurysms. *J Vasc Surg* 35 : 1289-91, 2002
5. Abu-Ghaida AM, Clair DG, Greenberg RK, Srivastava S, O'Hara PJ, Ouriel K : Broadening the applicability of endovascular aneurysm repair : the use of iliac conduits. *J Vasc Surg* 36 : 111-117, 2002

# Serum Hyaluronic Acid Concentration in Fontan Circulation: Correlation With Hepatic Function and Portal Vein Hemodynamics

Taiyu Hayashi · Ryo Inuzuka · Takahiro Shindo ·  
Yoichiro Hirata · Nobutaka Shimizu ·  
Akira Oka

Received: 25 July 2013 / Accepted: 3 October 2013 / Published online: 26 October 2013  
© Springer Science+Business Media New York 2013

**Abstract** Although liver fibrosis causes significant morbidity in the late postoperative period of the Fontan procedure, the diagnostic value of hyaluronic acid (HA), a serum marker of liver fibrosis, has not been established in Fontan patients. The purpose of this study was to determine whether increased serum HA concentration in Fontan patients is associated with an increase in inspiratory-to-expiratory flow rate ratio (Qin/Qex) of the portal vein (PV), which is indicative of liver fibrosis. We retrospectively studied 28 consecutive patients with Fontan circulation who underwent cardiac catheterisation for various indications. The median age at examination was 5.5 years (range 2.2–5.6). The median HA concentration was  $17.7 \text{ ng mL}^{-1}$  (range 10.0–82.1), which was used to divide our 28 patients into two groups. Patients in the high-HA group had significantly greater Qin/Qex of the PV than those in the low-HA group ( $1.25 \pm 0.12$  vs.  $1.12 \pm 0.11$ ,  $p < 0.05$ ). Platelet counts were significantly lower in the high-HA group ( $216 \pm 74$  vs.  $294 \pm 104 \times 10^9 \text{ L}^{-1}$ ,  $p < 0.05$ ). No significant difference was found in inferior vena caval pressure. In conclusion, increase of HA concentration in Fontan patients accompanies the change in PV hemodynamics peculiar to liver cirrhosis and might be an early indicator of liver fibrosis.

**Keywords** Fontan procedure · Liver fibrosis · Hyaluronic acid · Portal vein

Fontan circulation has become established as the definitive palliation in patients with a functionally univentricular

heart [10]. A chronically increased systemic venous pressure inherent in Fontan circulation leads to chronic hepatic congestion, which has a profibrotic effect and results in progressive sinusoidal collagen deposition in a perivenular distribution [23]. Along with the improved survival of patients with Fontan circulation, there is growing evidence that it is not uncommon for Fontan patients in the late postoperative period to develop liver fibrosis, even in the absence of a failing Fontan circulation, as has been shown in studies based on autopsy [11], biopsy specimens [17, 22], and radiological imaging [3, 4, 29].

Although the noninvasive diagnosis of liver fibrosis at an early stage is important, standard biochemical indices of liver hepatic dysfunction remain normal or only minimally increased, and no laboratory examination has been established as an indicator of liver fibrosis in patients with Fontan circulation [8, 16]. Hyaluronic acid (HA), a high molecular-weight glycosaminoglycan synthesized by mesenchymal cells, has been reported as a reliable marker that can predict liver fibrosis in children with various liver diseases [5, 12, 18]. However, the diagnostic value of serum HA concentration in patients with Fontan circulation remains to be determined.

The purpose of this study was to test the hypothesis that Fontan patients with increased serum HA concentration show changes in hepatic function test results and portal vein (PV) hemodynamics that are indicative of liver fibrosis or cirrhosis.

## Materials and Methods

We retrospectively reviewed 28 consecutive patients (14 males, 14 females) with Fontan circulation who underwent postoperative cardiac catheterisation for various indications at our

T. Hayashi (✉) · R. Inuzuka · T. Shindo · Y. Hirata ·  
N. Shimizu · A. Oka  
Department of Pediatrics, Graduate School of Medicine,  
University of Tokyo, Tokyo, Japan  
e-mail: taiyuhayashi@gmail.com

institution. All patients underwent laboratory investigations and echocardiographic evaluation before cardiac catheterisation. In addition, all patients were screened for ultrasonographic changes peculiar to liver cirrhosis, including surface nodularity of the liver and parenchymal heterogeneity [25]. The institutional Ethics Committee approved our retrospective study, and written informed consent was obtained from all patients.

### Laboratory Investigations

Serum levels of total bilirubin, aspartate aminotransferase (AST), alanine aminotransferase (ALT), cholinesterase, gamma-glutamyltranspeptidase, and total cholesterol were measured using standard methods. Coagulation tests were not included in the analysis because of the varied anticoagulant medication among our patients. Plasma brain natriuretic peptide concentration was measured by fluorescence-enzyme immunoassay (E test TOSOH II; Tosoh Corp., Tokyo, Japan). Serum HA was measured using a latex agglutination–turbidimetric immunoassay kit (LPIA Ace HA; Fujirebio Inc., Tokyo, Japan), the HA-detection limit of which is 10 ng mL<sup>-1</sup>. Although the normal adult value for serum HA is <50 ng mL<sup>-1</sup>, normal values in children have not been determined. Judging from previous reports, the upper limit of serum HA concentration in healthy children would not exceed 30 ng mL<sup>-1</sup> [12, 18]. In the current study, we divided our patients into two groups using the median value of serum HA concentration.

### Assessment of PV Hemodynamics by Ultrasonography

To assess PV hemodynamics, we calculated the inspiratory-to-expiratory flow rate ratio (Q<sub>in</sub>/Q<sub>ex</sub>) of the PV by using Doppler recordings [13–15]. Measurements were made with a Philips IE33 ultrasound system (Philips Medical Systems, Andover, MA) using a 5- or 8-MHz transducer. Respiratory and electrocardiography monitoring data were simultaneously recorded. Pulsed-wave Doppler recordings in the PV were obtained at the main portal trunk while the patient was breathing quietly in the supine position. The respiratory effect on mean flow rate of the PV was computed as previously described by Hsia et al. [13–15]. In brief, the velocity time integral (VTI) for the inspiratory phase (VTI<sub>in</sub>) and the expiratory phase (VTI<sub>ex</sub>) of the respiratory cycle was evaluated, as well as the time interval for inspiration (T<sub>in</sub>) and expiration (T<sub>ex</sub>) (Fig. 1). In patients with Fontan circulation, it can be assumed that the cross-sectional area of the PV (A) is constant through respiration owing to the high venous pressure. Therefore, the mean flow rate during the inspiratory phase (Q<sub>in</sub>) and the expiratory phase (Q<sub>ex</sub>) could be calculated by using the following equations:

$$Q_{in} = VTI_{in} * A / T_{in}, \quad Q_{ex} = VTI_{ex} * A / T_{ex}$$

The effect of respiration on flow rate was expressed as the Q<sub>in</sub>/Q<sub>ex</sub>:

$$Q_{in}/Q_{ex} = (VTI_{in}/T_{in}) * (T_{ex}/VTI_{ex})$$

The Q<sub>in</sub>/Q<sub>ex</sub> values of the PV were measured from three full respiratory cycles, and the results for each of the measurements were averaged. All measurements were performed by one of the researchers who was blinded to the clinical data of the patient.

### Cardiac Catheterization

All patients underwent cardiac catheterisation with intravenous anaesthesia and maintained spontaneous respiration on ambient air. The hemodynamic data obtained included inferior vena caval pressure and end-diastolic pressure of the systemic ventricle. The Nakata index was also measured during cardiac catheterisation.

### Statistical Analysis

Data are expressed as frequencies, means ± SDs, or as medians and ranges as appropriate. Differences in the categorical variables between groups were tested with Fisher’s exact test. Differences in the continuous variables were analyzed by Mann–Whitney *U* test. A *p*-value of <0.05 was considered statistically significant. All analyses were performed using R version 2.13.0.

## Results

### Patient Characteristics

The demographic characteristics of our patients are listed in Table 1. The median age at cardiac catheterisation was 5.5 years (range 2.2–25.6), and the median time interval

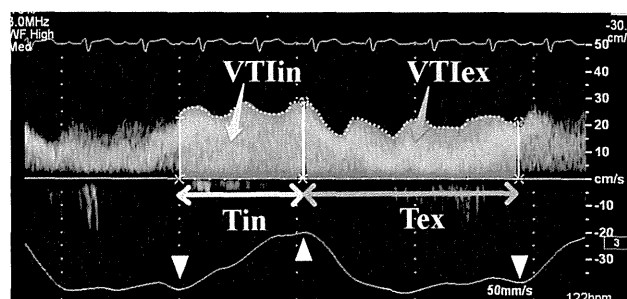


**Fig. 1** Pulsed-wave Doppler recording of portal venous flow. The tracing at the bottom is the simultaneous respiratory recording, which allowed distinguishing the onset of the inspiratory phase (downward-pointing arrowheads) and the expiratory phase (upward-pointing arrowhead). For flow rate calculation, we measured VTI<sub>in</sub> and VTI<sub>ex</sub> as well as T<sub>in</sub> and T<sub>ex</sub>

between the Fontan procedure and cardiac catheterisation was 2.2 years (range 0.3–20.0). Fontan procedures without fenestration (26 extracardiac conduit, 1 lateral tunnel, and 1 atriopulmonary connection) were performed at a median patient age of 2.3 years (range 1.6–8.4). Of 26 patients with extracardiac conduit, 3 underwent emergent creation of fenestration within 48 hours after the Fontan procedure. At cardiac catheterisation, 25 patients (89 %) were in New York Heart Association (NYHA) functional class I, and 3 patients (11 %) were in NYHA functional class II. All patients were in sinus rhythm except for 1 patient (patient no. 23) who had intra-atrial re-entrant tachycardia. Cardiac catheterisation measurements were unavailable for this patient because he underwent catheter ablation for the intra-atrial re-entrant tachycardia, and pressure study was not performed. Inferior vena caval pressure was not measured in another patient (patient no. 16) because of an interrupted inferior vena cava. None of the patients had other known causes of liver diseases, such as hepatitis B, hepatitis C, autoimmune hepatitis, and drug-induced liver injury. On abdominal ultrasonography, none of the patients showed evidence of liver cirrhosis.

#### Comparison Between High- and Low-HA Groups

The median value of serum HA concentration was  $17.7 \text{ ng mL}^{-1}$  (range 10.0–82.1), which was used to divide our 28 patients into two groups (i.e., low-HA group and high-HA group). By definition, serum HA concentration was significantly increased in the high-HA group [median  $29.3 \text{ ng mL}^{-1}$  (range 18.4–82.1) vs. median  $11.0 \text{ ng mL}^{-1}$  (range 10.0–17.0), respectively;  $p < 0.0001$ ]. Patient characteristics, laboratory data, and hemodynamic measurements for both groups are listed in Table 2.

Patient ages at examination and at Fontan procedure, as well as time interval since Fontan, were not different between the low- and the high-HA groups. There was no significant difference in patient body weight and oxygen saturation under ambient air. All of the three patients with NYHA functional class II belonged to the high-HA group.

Laboratory examination showed that platelet counts were significantly decreased in the high-HA group ( $216 \pm 74$  vs.  $294 \pm 104 \times 10^9 \text{ L}^{-1}$ , respectively;  $p < 0.05$ ). Regarding the other indices of hepatic function, there was no significant difference in the serum level of total bilirubin, AST, ALT, cholinesterase, gamma-glutamyltranspeptidase, and total cholesterol between the low and high HA groups. There was also no significant difference in plasma brain natriuretic peptide concentration between the two groups. The degree of aortic regurgitation and atrioventricular regurgitation was similar in the two groups.

Although inferior vena caval pressure tended to be greater in the high-HA group, the difference did not reach statistical significance. Other cardiac catheterisation measurements, including end-diastolic pressure of the systemic ventricle and the Nakata index, were similar in the two groups.

Flow rate calculations of the PV showed that patients in the high-HA group had significantly increased  $Q_{in}/Q_{ex}$  of the PV compared with those in the low-HA group ( $1.25 \pm 0.12$  vs.  $1.12 \pm 0.11$ , respectively;  $p < 0.05$ , Fig. 2a). In addition, statistical significance was maintained even after we confined the analysis to patients with inferior vena caval pressure  $< 15 \text{ mmHg}$  ( $Q_{in}/Q_{ex}$  of the PV,  $1.22 \pm 0.08$  for the high-HA group vs.  $1.10 \pm 0.09$  for the low-HA group;  $p < 0.05$ , Fig. 2b).

#### Discussion

We found that in Fontan patients of NYHA functional class I and II, high serum HA concentration was associated with decreased platelet count and pronounced inspiratory augmentation of the portal venous flow rate. Our results suggested that increase of serum HA concentration in Fontan patients accompanies a change in PV hemodynamics similar to that in patients with cirrhosis of the liver, and therefore, it might be an early indicator of liver fibrosis.

#### HA as a Marker of Liver Fibrosis

Our patients, all of whom were in hemodynamically stable Fontan circulation with NYHA functional class I and II, showed varied serum HA concentrations ranging from 10.0 to  $82.1 \text{ ng mL}^{-1}$ . HA acid is a component of the extracellular matrix, and liver fibrosis stimulates the synthesis of HA in hepatic mesenchymal cells. At the same time, the clearance of HA from circulation is impaired owing to the decreased permeability of the sinusoidal endothelial cells in the presence of liver fibrosis [9]. Several studies previously showed that serum HA concentration predicted liver fibrosis in adult patients with chronic hepatitis [27, 30] as well as in pediatric patients with nonalcoholic fatty liver disease [18], beta-thalassemia major [5], and various liver diseases [12].

Although the normal values in children and changes with advancing age have not been confirmed for serum HA concentration, a previous study reported that the normal value for HA in children was  $< 30 \text{ ng mL}^{-1}$  [12]. Another study in children with nonalcoholic fatty liver disease showed that the median serum HA concentration in patients with biopsy-confirmed liver fibrosis was  $20.5 \text{ ng mL}^{-1}$  (interquartile range 19.5–34.8) [18], which was significantly greater than that in patients without fibrosis. Therefore, we

**Table 1** Demographic characteristics of patients

Patient	Sex	Age (years)	Time since Fontan (years)	Diagnosis	Fontan type	NYHA functional class	Serum HA (ng mL <sup>-1</sup> )	Qin/Qex of the PV	IVC pressure (mmHg)
1	Male	3.2	1.0	TA	EC	I	<10.0	1.00	12
2	Male	4.3	1.0	HLHS	EC with fenestration	I	<10.0	1.14	12
3	Female	3.4	1.3	SRV	EC	I	<10.0	1.27	16
4	Female	3.3	0.9	SLV	EC	I	<10.0	1.19	9
5	Male	3.2	0.9	TGA	EC	I	<10.0	0.98	11
6	Female	6.5	4.2	HLHS variant	EC	I	<10.0	1.10	10
7	Male	5.7	1.2	HLHS	EC	I	10.6	0.96	14
8	Male	8.0	4.2	SRV	EC	I	11.3	1.10	12
9	Male	16.9	12.6	SLV	EC	I	11.9	1.05	13
10	Female	2.8	0.3	SRV	EC	I	14.9	1.24	10
11	Male	8.8	6.3	PA/IVS	EC	I	15.3	1.13	12
12	Female	2.2	0.5	DORV, PA, MS	EC with fenestration	I	15.6	1.18	11
13	Male	5.8	3.8	DILV	EC	I	15.6	1.10	9
14	Female	3.2	0.9	SRV	EC	I	17.0	1.30	15
15	Male	3.2	1.2	SRV	EC	I	18.4	1.23	15
16	Male	19.0	10.8	SRV	EC	I	21.1	0.97	NA
17	Male	6.8	2.9	Hypoplastic RV, TS, PS	EC	I	22.7	1.25	9
18	Male	3.8	0.4	SRV	EC	I	24.3	1.28	13
19	Female	5.3	2.4	SLV	EC	I	24.4	1.18	20
20	Female	4.0	2.0	HLHS	EC	I	25.2	1.06	12
21	Female	6.2	4.6	SRV	EC with fenestration	I	27.1	1.29	16
22	Female	19.4	10.9	DILV	EC	II	31.5	1.27	12
23	Male	25.8	19.7	TA	APC	II	31.6	1.38	NA
24	Female	13.1	11.2	SRV	EC	I	33.4	1.48	16
25	Female	2.3	0.3	SRV	EC	I	38.1	1.26	11
26	Female	7.5	5.3	SRV	EC	I	45.1	1.22	12
27	Male	15.3	9.9	PA/IVS	LT	II	50.7	1.24	16
28	Female	2.4	0.5	HLHS	EC	I	82.1	1.33	18

APC atriopulmonary connection, DILV double-inlet left ventricle, DORV double-outlet right ventricle, EC extracardiac conduit, HLHS hypoplastic left heart syndrome, IVC inferior vena cava, LT lateral tunnel, MS mitral stenosis, NA not available, PA pulmonary atresia, PA/IVS pulmonary atresia with intact ventricular septum, PS pulmonary stenosis, RV right ventricle, SLV single left ventricle, SRV single right ventricle, TA tricuspid atresia, TGA transposition of the great arteries, TS tricuspid stenosis

considered that the serum HA concentrations [median 29.3 ng mL<sup>-1</sup> (range 18.4–82.1)] in the high-HA group had clinical relevance and that it was reasonable to compare the two groups that were divided at the median value of serum HA concentration.

#### HA and PV Hemodynamics

Our study showed that Fontan patients with increased serum HA concentration had pronounced inspiratory augmentation of the portal venous flow rate. This alteration in PV hemodynamics is considered to represent fibrotic change of the liver.

In the normal population, portal venous flow decreases during inspiration as the descending diaphragm compresses the compliant and easily collapsible portal venules and

hepatic sinusoids [19]. As a result, the Qin/Qex of the PV is <1 in the normal population [13]. Because the cirrhotic liver is firmer and less collapsible than the normal liver, the decrease in portal venous flow during inspiration becomes less prominent: A previous study with magnetic resonance imaging showed that maximal inspiration caused a 13.5 % decrease in PV flow in cirrhotic patients compared with a 24.6 % decrease in healthy controls [24].

In Fontan patients, more blood flow is observed in the PV during inspiration than during expiration [13], and the Qin/Qex of the PV is  $\geq 1$ . The chronically increased central venous pressure inherent in Fontan circulation leads to hepatic congestion, increased sinusoidal pressure, and decreased hepatic compressibility. As a result, sinusoids remain patent during inspiration and act as fluid-filled tubes. Because most of the hepatic venous flow is driven during inspiration, portal



**Table 2** Clinical characteristics, laboratory data, and hemodynamic measurements of the low- and high-HA groups

Variables	Low-HA group (n = 14)	High-HA group (n = 14)	p
HA (ng mL <sup>-1</sup> )	11.0 (10.0–17.0) <sup>a</sup>	29.3 (18.4–82.1)	<0.0001*
Age at examination (years)	3.9 (2.2–17.0)	6.5 (2.3–25.6)	0.18
Age at Fontan procedure (years)	2.3 (1.7–4.5)	2.4 (1.6–8.4)	0.98
Interval since Fontan procedure (years)	1.1 (0.3–12.6)	3.8 (0.3–19.7)	0.17
Body weight at examination (kg)	13.8 (9.5–53.2)	19.1 (11.0–70.9)	0.1
SpO <sub>2</sub> ≥ 92	13 (93 %)	10 (71 %)	0.32
SpO <sub>2</sub> < 92	1 (7 %)	4 (29 %)	
NYHA functional class I	14 (100 %)	11 (79 %)	0.22
NYHA functional class II	0	3 (21 %)	
Degree of aortic regurgitation			
None	10 (71 %)	9 (64 %)	1
Mild	4 (29 %)	5 (36 %)	
Degree of atrioventricular valve regurgitation			
None	9 (64 %)	9 (64 %)	0.43
Mild	3 (22 %)	5 (36 %)	
Moderate	2 (14 %)	0 (0 %)	
T-Bil (mg dL <sup>-1</sup> )	0.7 (0.5–1.4)	0.7 (0.4–5.4)	0.85
AST (IU L <sup>-1</sup> )	37.1 ± 7.8	36.4 ± 11.8	0.42
ALT (IU L <sup>-1</sup> )	21.4 ± 5.4	22.1 ± 8.6	0.87
ChE (IU L <sup>-1</sup> )	314 (214–547)	279 (209–361)	0.21
GGTP (IU L <sup>-1</sup> )	47 (22–205)	53.5 (22–161)	0.18
T-Chol (mg dL <sup>-1</sup> )	126.9 ± 24.9	120.0 ± 21.1	0.48
Platelet count (×10 <sup>9</sup> L <sup>-1</sup> )	294 ± 104	216 ± 74	<0.05*
Plasma BNP level (pg mL <sup>-1</sup> )	11.0 (4.9–59.3)	25.2 (4.0–163.3)	0.51
Qin/Qex of the PV	1.12 ± 0.11	1.25 ± 0.12	<0.05*
IVC mean pressure (mmHg)	11.9 ± 2.1	14.2 ± 3.2 <sup>b</sup>	0.054
<15	12 (86 %)	6 (43 %)	0.058
≥15	2 (14 %)	6 (43 %)	
Unknown	0	2 (14 %)	
End-diastolic pressure of the systemic ventricle (mmHg)	6.0 ± 1.9	7.1 ± 1.9 <sup>c</sup>	0.27
Nakata index (mm <sup>2</sup> m <sup>-2</sup> )	205 ± 55	197 ± 89 <sup>c</sup>	0.53

BNP brain natriuretic peptide, ChE cholinesterase, GGTP gamma-glutamyltranspeptidase, IVC inferior vena cava, SpO<sub>2</sub> percutaneous oxygen saturation, T-Bil total bilirubin, T-Chol total cholesterol, ALT alanine aminotransferase, AST aspartate aminotransferase

\* Statistically significant

<sup>a</sup> Data are presented as means ± SDs, medians (ranges), or n (%)

<sup>b</sup> Data are available in 12 patients

<sup>c</sup> Data are available in 13 patients

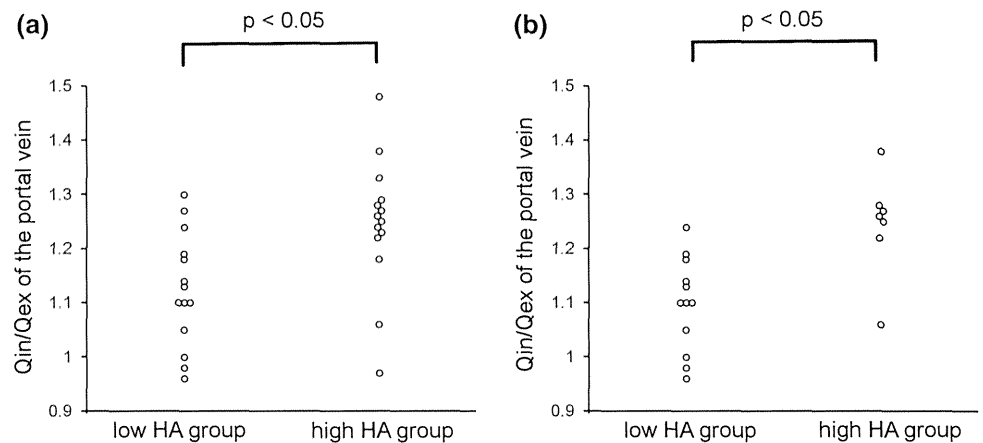
venous flow becomes dominant during inspiration in concert with an increased hepatic venous flow [13].

In Fontan patients with fibrotic change of the liver, portal venules and hepatic sinusoids would become even less collapsible, and inspiratory augmentation of the portal venous flow would be more prominent. Therefore, the significantly greater Qin/Qex of the PV observed in our high-HA patients indicates fibrotic change of the liver. The significantly lower platelet counts support the presence of liver fibrosis in the high-HA group considering that thrombocytopenia is a common feature of chronic liver disease [2]. Our results

suggested that increase of serum HA concentration in Fontan patients might be useful as an indicator of liver fibrosis.

PV hemodynamics could also be influenced by factors other than fibrotic change of the liver. It has been well described that the inspiratory augmentation of portal venous flow becomes more prominent in patients with functionally poorer Fontan circulation [14]. The study by Hsia et al. [14] showed that the Qin/Qex of the PV was significantly increased in Fontan patients with inferior vena caval pressure ≥15 mmHg than in those with inferior vena caval pressure <15 mmHg (1.4 ± 0.5 vs.

**Fig. 2** Scatter plots of  $Q_{in}/Q_{ex}$  of the PV according to serum HA concentration for all patients in our series (a) and those with inferior vena caval pressure <15 mmHg (b)



$1.0 \pm 0.3$ ,  $p < 0.05$ ). The same trend was also observed in patients with NYHA functional class III/VI compared with those with class I/II ( $1.3 \pm 0.5$  vs.  $1.0 \pm 0.3$ ,  $p < 0.05$ ).

In our patients, inferior vena caval pressure might also have affected PV hemodynamics. However, inferior vena caval pressure did not differ significantly between the low- and high-HA groups. In addition, the statistical significance of the difference of the PV hemodynamics was maintained even after we confined the analysis to patients with inferior vena caval pressure <15 mmHg. Therefore, we attributed the difference in PV hemodynamics to the presence of liver fibrosis.

#### Liver Fibrosis in Fontan Circulation

Along with the improved survival of patients with Fontan circulation, much attention has been paid recently to liver fibrosis in Fontan patients [21]. Previous reports suggested that patients with a failing Fontan circulation, who also had markedly increased systemic venous pressure, were at risk of developing liver fibrosis [11, 17]. However, there is growing evidence that liver fibrosis is frequently observed among Fontan patients in the late postoperative period [3, 4, 22, 29]. Liver fibrosis would cause significant morbidity and mortality in Fontan patients. Fontan-associated liver fibrosis could ultimately result in hepatocellular carcinoma [11]. A high perioperative mortality rate was reported in Fontan patients with cirrhosis who underwent surgical conversion to total cavopulmonary connection [1]. Although the noninvasive diagnosis of liver fibrosis at an early stage is important, Fontan-associated liver disease appears to develop slowly and subclinically in most patients [21], and the standard biochemical indices of liver hepatic dysfunction remains normal or only minimally increased in Fontan patients [23]. Some reports pointed to the applicability of noninvasive liver function tests for the longitudinal assessment of hepatic function in Fontan

patients, such as gamma-glutamyltranspeptidase level [16, 20] and type IV collagen 7 s domain level [8, 20]. Although scoring systems, including the Forns index [6], the FIB-4 index [26], and AST-to-platelet ratio index [28], have been reported to be useful in predicting hepatitis-induced liver fibrosis in adults, few studies have delved into the diagnostic utility of these indices in children or patients with Fontan circulation [3].

In our present study, none of the Fontan patients had ultrasonographic changes peculiar to liver cirrhosis, including surface nodularity of the liver and parenchymal heterogeneity. In addition, the results of routine hepatic function tests remained almost normal in many patients. Nonetheless, Fontan patients with increased serum HA concentration had alteration in PV hemodynamics that was characteristic of liver fibrosis, which highlights the diagnostic value of serum HA concentration as an early indicator of liver fibrosis.

It is of note that the high serum HA group contained three very young children who had undergone a Fontan procedure just several months before the examination. Considering that liver fibrosis is a late postoperative complication of the Fontan procedure, it was unlikely for these young patients who had undergone Fontan procedure <1 year ago would develop full-fledged liver fibrosis. Although we speculated that the increased serum HA concentration in these young patients might reflect a sub-clinical fibrotic change of the liver, longitudinal follow-up is required to determine the clinical relevance of the increased serum HA concentration in such an early postoperative period of the Fontan procedure.

#### Study Limitations

Our study had limitations that must be addressed. First, none of our patients underwent liver biopsy, which is considered the “gold standard” for the assessment of liver fibrosis. However, liver biopsy is invasive and prone to

sampling errors and interobserver variability [7]. In addition, radiological imaging examination was not performed in our patients because no abnormalities were detected by the liver enzyme tests and abdominal ultrasonographic screening. Recent studies showed that computed tomography and magnetic resonance imaging could identify hepatic abnormalities in Fontan patients that were unrecognizable by standard laboratory examinations [4, 29]. However, these abnormalities in radiological images were identified in patients at median ages of 14.4 years [4] and 18.9 years [29] and therefore were older than our patients. Thus, we considered that it would be less likely for our patients to show hepatic lesions on radiological images and adopted portal venous hemodynamics as an indicator of liver fibrosis.

Second, this study was not intended for establishing cut-off values for predicting liver fibrosis in Fontan patients. Aiming at evaluating the relationship between serum HA concentration and liver fibrosis, we divided our patients into two groups using the median value of serum HA concentration. As a result, three young adult patients were classified in the high-HA group despite that their serum HA concentration did not exceed the upper limit of normal for adults ( $50 \text{ ng mL}^{-1}$ ). Because this is a retrospective cross-sectional study including a small number of patients, further investigation with a larger population and a longer follow-up, including radiological imaging examinations, is required to determine the clinical ramifications of increase in serum HA concentration.

In conclusion, Fontan patients with increased serum HA concentration had lower platelet count and pronounced inspiratory augmentation of the portal venous flow rate. Increase of serum HA concentration in Fontan patients accompanies the change in PV hemodynamics similar to that in patients with cirrhosis of the liver. Serum HA concentration might be an early indicator of liver fibrosis, although further investigation with a larger population and longer follow-up is required to determine its clinical implications.

**Acknowledgment** This study was supported by the Japan Society for the Promotion of Science Grant-in-Aid (KAKENHI) No. 23659515.

## References

- Aboulhosn J, Williams R, Shivkumar K, Barkowski R, Plunkett M, Miner P (2010) Arrhythmia recurrence in adult patients with single ventricle physiology following surgical Fontan conversion. *Congenit Heart Dis* 5:430–434
- Amitrano L, Guardascione MA, Brancaccio V, Balzano A (2002) Coagulation disorders in liver disease. *Semin Liver Dis* 22:83–96
- Baek JS, Bae EJ, Ko JS, Kim GB, Kwon BS, Lee SY et al (2010) Late hepatic complications after Fontan operation; non-invasive markers of hepatic fibrosis and risk factors. *Heart* 96:1750–1755
- Bulut OP, Romero R, Mahle WT, McConnell M, Braithwaite K, Shehata BM et al (2013) Magnetic resonance imaging identifies unsuspected liver abnormalities in patients after the Fontan procedure. *J Pediatr* 163:201–206
- El-Shabrawi MH, Zein El Abedin MY, Omar N, Kamal NM, Elmakarem SA et al (2012) Predictive accuracy of serum hyaluronic acid as a non-invasive marker of fibrosis in a cohort of multi-transfused Egyptian children with beta-thalassaemia major. *Arab J Gastroenterol* 13:45–48
- Forns X, Ampurdanès S, Llovet JM, Aponte J, Quintó L, Martínez-Bauer E et al (2002) Identification of chronic hepatitis C patients without hepatic fibrosis by a simple predictive model. *Hepatology* 36:986–992
- Friedrich-Rust M, Koch C, Rentzsch A, Sarrazin C, Schwarz P, Herrmann E (2008) Noninvasive assessment of liver fibrosis in patients with Fontan circulation using transient elastography and biochemical fibrosis markers. *J Thorac Cardiovasc Surg* 135:560–567
- Furukawa T, Akimoto K, Ohtsuki M, Sato K, Suzuki M, Takahashi K et al (2011) Non-invasive assessment of liver fibrosis in patients after the Fontan operation. *Pediatr Int* 53:980–984
- George J, Tsutsumi M, Takase S (2004) Expression of hyaluronic acid in *N*-nitrosodimethylamine induced hepatic fibrosis in rats. *Int J Biochem Cell Biol* 36:307–319
- Gewillig M (2005) The Fontan circulation. *Heart* 91:839–846
- Ghaferi AA, Hutchins GM (2005) Progression of liver pathology in patients undergoing the Fontan procedure: chronic passive congestion, cardiac cirrhosis, hepatic adenoma, and hepatocellular carcinoma. *J Thorac Cardiovasc Surg* 129:1348–1352
- Hartley JL, Brown RM, Tybulewicz A, Hayes P, Wilson DC, Gillett P et al (2006) Hyaluronic acid predicts hepatic fibrosis in children with hepatic disease. *J Pediatr Gastroenterol Nutr* 43:217–221
- Hsia TY, Khambadkone S, Redington AN, Migliavacca F, Deanfield JE, de Leval MR (2000) Effects of respiration and gravity on infradiaphragmatic venous flow in normal and Fontan patients. *Circulation* 102(Suppl 3):III148–III153
- Hsia TY, Khambadkone S, Deanfield JE, Taylor JF, Migliavacca F, De Leval MR (2001) Subdiaphragmatic venous hemodynamics in the Fontan circulation. *J Thorac Cardiovasc Surg* 121:436–447
- Hsia TY, Khambadkone S, Redington AN, de Leval MR (2001) Effect of fenestration on the sub-diaphragmatic venous hemodynamics in the total-cavopulmonary connection. *Eur J Cardiothorac Surg* 19:785–792
- Kaulitz R, Haber P, Sturm E, Schäfer J, Hofbeck M (2013) Serial evaluation of hepatic function profile after Fontan operation. *Herz*. doi:10.1007/s00059-013-3811-5
- Kiesewetter CH, Sheron N, Vettukattill JJ, Hacking N, Stedman B, Millward-Sadler H et al (2007) Hepatic changes in the failing Fontan circulation. *Heart* 93:579–584
- Lebensztejn DM, Wierzbicka A, Socha P, Pronicki M, Skiba E, Werpachowska I et al (2011) Cytokeratin-18 and hyaluronic acid levels predict liver fibrosis in children with non-alcoholic fatty liver disease. *Acta Biochim Pol* 58:563–566
- Moreno AH, Burchell AR (1982) Respiratory regulation of splanchnic and systemic venous return in normal subjects and in patients with hepatic cirrhosis. *Surg Gynecol Obstet* 154:257–267
- Oka T, Kato R, Fumino S, Toiyama K, Yamagishi M, Itoi T (2013) Noninvasive estimation of central venous pressure after Fontan procedure using biochemical markers and abdominal echography. *J Thorac Cardiovasc Surg* 146:153–157
- Rychik J, Veldtman G, Rand E, Russo P, Rome JJ, Krok K (2012) The precarious state of the liver after a Fontan operation: summary of a multidisciplinary symposium. *Pediatr Cardiol* 33:1001–1012
- Schwartz MC, Sullivan LM, Glatz AC, Rand E, Russo P, Goldberg DJ et al (2013) Portal and sinusoidal fibrosis are common on liver biopsy after Fontan surgery. *Pediatr Cardiol* 34:135–142

23. Shah H, Kuehl K, Sherker AH (2010) Liver disease after the Fontan procedure: what the hepatologist needs to know. *J Clin Gastroenterol* 44:428–431
24. Sugano S, Yamamoto K, Sasao K, Watanabe M (1999) Portal venous blood flow while breath-holding after inspiration or expiration and during normal respiration in controls and cirrhotics. *J Gastroenterol* 34:613–618
25. Tchelepi H, Ralls PW, Radin R, Grant E (2002) Sonography of diffuse liver disease. *J Ultrasound Med* 21:1023–1032
26. Vallet-Pichard A, Mallet V, Nalpas B, Verkarre V, Nalpas A, Dhalluin-Venier V et al (2007) FIB-4: an inexpensive and accurate marker of fibrosis in HCV infection. Comparison with liver biopsy and fibrotest. *Hepatology* 46:32–36
27. Valva P, Casciato P, Diaz Carrasco JM, Gadano A, Galdame O, Galoppo MC (2011) The role of serum biomarkers in predicting fibrosis progression in pediatric and adult hepatitis C virus chronic infection. *PLoS One* 6:e23218
28. Wai CT, Greenson JK, Fontana RJ, Kalbfleisch JD, Marrero JA, Conjeevaram HS et al (2003) A simple noninvasive index can predict both significant fibrosis and cirrhosis in patients with chronic hepatitis C. *Hepatology* 38:518–526
29. Wallihan DB, Podberesky DJ (2013) Hepatic pathology after Fontan palliation: spectrum of imaging findings. *Pediatr Radiol* 43:330–338
30. Xie SB, Yao JL, Zheng RQ, Peng XM, Gao ZL (2003) Serum hyaluronic acid, procollagen type III and IV in histological diagnosis of liver fibrosis. *Hepatobiliary Pancreat Dis Int* 2:69–72

# Massive tricuspid regurgitation due to pacemaker-lead puncture of the tricuspid valve: successful diagnosis by 3-dimensional echocardiography

Rina Tamai · Tomoya Hara · Hirotsugu Yamada · Susumu Nishio ·  
Mika Bando · Junko Hotchi · Shuji Hayashi · Toshiyuki Niki ·  
Tetsuya Kitagawa · Masataka Sata

Received: 29 January 2013 / Accepted: 12 April 2013 / Published online: 31 May 2013  
© The Japan Society of Ultrasonics in Medicine 2013

**Abstract** An 83-year-old woman presented to our echocardiographic center with symptoms of right heart failure. A dual-chamber DDDR pacemaker had been implanted 9 years earlier. Two-dimensional echocardiography revealed right atrial and ventricular enlargement and massive tricuspid regurgitation with immobilization of the anterior leaflet of the tricuspid valve. Three-dimensional transesophageal echocardiography showed that the pacemaker lead had punctured the leaflet. These echocardiographic findings were confirmed during surgery. The pacemaker lead was transected and removed, and pericardial patch closure of the leaflet hole and tricuspid annuloplasty were performed. The mechanism of regurgitation was elucidated by real-time three-dimensional echocardiography, and surgical repair was straightforward.

**Keywords** Pacemaker-lead puncture · Tricuspid regurgitation · 3-Dimensional echocardiography

## Introduction

Tricuspid valve perforation by pacemaker lead is an extremely rare complication of transvenous pacemaker implantation. Damage to the tricuspid valve caused by pacemaker lead may result in severe symptomatic tricuspid regurgitation and may not be overtly visualized by echocardiography. We report a case of a patient with severe tricuspid valve regurgitation due to tricuspid valve perforation by pacemaker lead. In our case, the mechanism of regurgitation was elucidated by real-time three-dimensional echocardiography, and surgical repair was straightforward.

## Case report

An 83-year-old woman was referred to our ultrasound examination center with 2-week history of increasing M. Sata  
e-mail: masataka.sata@tokushima-u.ac.jp

H. Yamada · S. Nishio · S. Hayashi · M. Sata  
Ultrasound Examination Center, Tokushima University Hospital,  
Tokushima, Japan  
e-mail: nishio0909@yahoo.co.jp

S. Hayashi  
e-mail: kiwamihe@gmail.com

T. Kitagawa  
Department of Cardiovascular Surgery, Tokushima University  
Hospital, Tokushima, Japan  
e-mail: kitagawa@clin.med.tokushima-u.ac.jp

**Electronic supplementary material** The online version of this article (doi:10.1007/s10396-013-0459-y) contains supplementary material, which is available to authorized users.

R. Tamai · T. Hara · H. Yamada (✉) · M. Bando · J. Hotchi ·  
T. Niki · M. Sata  
Department of Cardiovascular Medicine, Tokushima University  
Hospital, 2-50-1 Kuramoto-cho, Tokushima 770-8503, Japan  
e-mail: yamadah@tokushima-u.ac.jp

R. Tamai  
e-mail: tamai831@gmail.com

T. Hara  
e-mail: itumo-kimiwo-mitumeteru@hotmail.co.jp

M. Bando  
e-mail: banban6541@yahoo.co.jp

J. Hotchi  
e-mail: jhotchi@clin.med.tokushima-u.ac.jp

T. Niki  
e-mail: ninnindesi@yahoo.co.jp

orthopnea, ankle swelling, and abdominal distension. A dual-chamber pacemaker had been implanted due to sick sinus syndrome 9 years earlier. She had been on oral diuretic therapy for 1 year. She had a regular pulse of 70 beats per minute and her blood pressure was 98/64 mmHg. Her jugular vein was dilated, and pitting edema to the mid calves was observed. A 3/6 grade pansystolic murmur was heard along the left sternal border. A chest X-ray showed cardiomegaly and bilateral pleural effusion. Electrocardiogram (ECG) showed all DDD pacing rhythm. These clinical findings were suggestive of right heart failure.

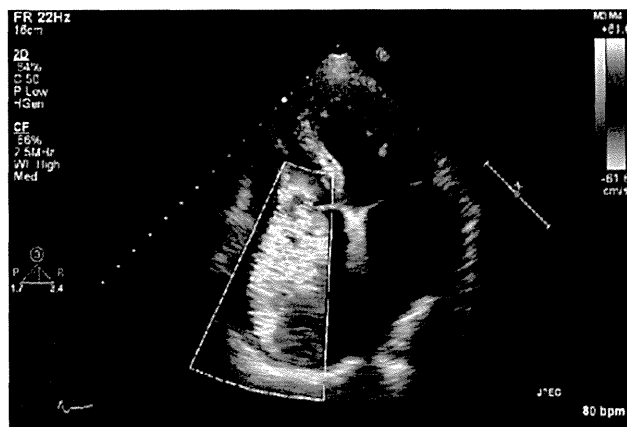


**Fig. 1** Transthoracic echocardiography (apical four-chamber view). Color Doppler mapping shows massive tricuspid regurgitation due to immobilization of the anterior leaflet of the tricuspid valve

Two-dimensional echocardiography showed right atrial and ventricular enlargement and massive tricuspid regurgitation (TR) with immobilization of the anterior leaflet of the tricuspid valve (Fig. 1; Video 1). Three-dimensional transesophageal echocardiography revealed that the pacemaker lead had punctured the leaflet (Fig. 2a; Video 2). This phenomenon was confirmed by observation of a two-dimensional echocardiogram reconstructed from the three-dimensional dataset (Fig. 3).

Open heart surgery was performed because medical treatment failed to cure heart failure. The leaflet was found to be punctured by the pacemaker lead, the distal portion of which was fixed to the right ventricular myocardium by surrounding scar tissue (Fig. 2b). The pacemaker lead was transected and removed, and pericardial patch closure of the leaflet hole and tricuspid annuloplasty were performed. Two bipolar epicardial pacemaker leads were placed and connected to the new generator. The patient tolerated the procedure well and was discharged on postoperative day 40.

## Discussion

Tricuspid valve perforation by pacemaker lead is an extremely rare complication of transvenous pacemaker implantation. Lin et al. [1] published a report of 41 patients with pacemaker-lead-related TR. They found perforation of the tricuspid valve leaflet in seven patients, and lead

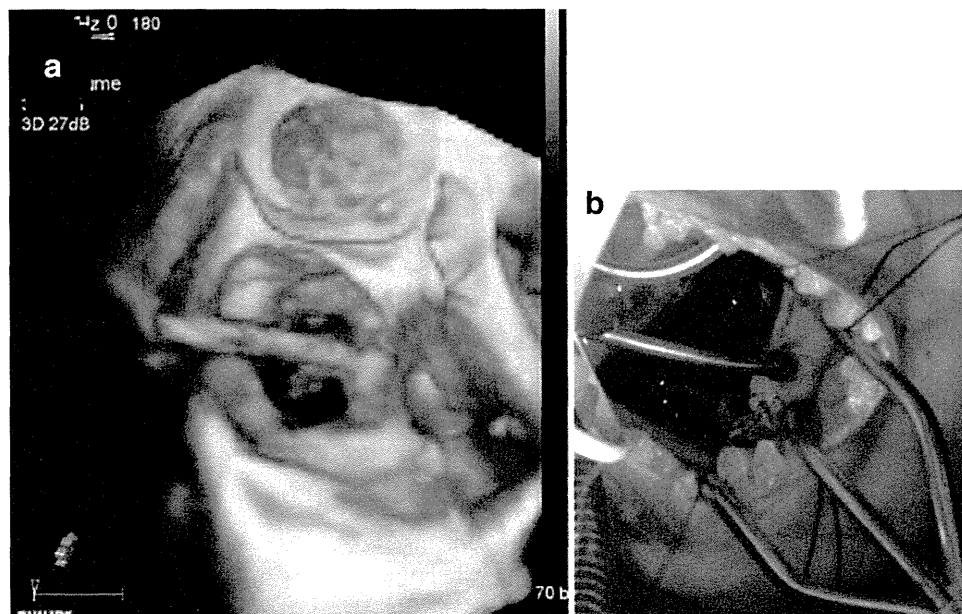


**Fig. 2** a Real-time three-dimensional echocardiography (transesophageal echocardiographic view from the right atrium to the right ventricle) showing the anterior leaflet penetrated by the pacemaker lead. b Intraoperative photograph demonstrating a similar view to the echocardiographic picture

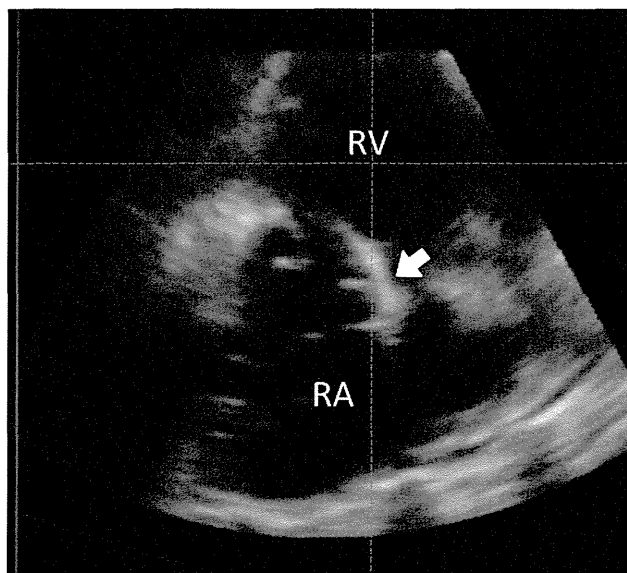


**Fig. 3** Two-dimensional echocardiogram reconstructed from 3-dimensional dataset. The *arrow* indicates the portion of the tricuspid valve anterior leaflet penetrated by the pacemaker lead

entanglement, impingement, and adherence to the tricuspid valve in four, 16, and 14 patients, respectively. A total of 22 patients in their study underwent tricuspid valve replacement, while tricuspid valve repair was performed in the remaining 19 patients. The investigators observed no repeat surgery for recurrent TR after mean follow-up of 8.2 years. However, echocardiographic data regarding postoperative residual or recurrent TR were not presented.

As in the present case, the mechanism of pacemaker-lead-related TR could not be elucidated by 2-dimensional echocardiography. Lin et al. [1] reported that the mechanism of TR could be diagnosed preoperatively in only five of the 41 patients. On the other hand, Seo et al. [2] evaluated 87 patients with pacemaker-lead-related TR using 3-dimensional echocardiography. In 82 patients, 3-dimensional echocardiography revealed the lead route and location at the tricuspid valve. Three-dimensional echocardiography can also be used to reconstruct unique views from collected volume data that cannot be obtained by 2-dimensional echocardiography. In the present case, real-time 3-dimensional echocardiography suggested puncture of the anterior

leaflet (Fig. 2a; Video 2), and reconstructed 2-dimensional views confirmed the path of the lead through the middle portion of the anterior leaflet, not in the commissures (Fig. 3).

In this case, her pacemaker was implanted at another hospital and she was followed up for a long time at that institution. Therefore, detailed information on the time course of development of TR was not available. Although leaflet penetration occurred immediately after implantation, early TR is often minimal, and the problem was not diagnosed acutely. It took 8 years from her pacemaker implantation to develop severe symptoms of heart failure, and it took another year to become resistant to medication. The likely mechanism for this long time lag may be slow progression of right atrial and ventricular enlargement. Several adjustments of her medication and pacemaker settings were made out of consideration for the risks associated with invasive surgery, but open heart surgery was ultimately necessary.

According to the data from Seo et al. [2], the location of the pacemaker lead in relation to the tricuspid valve can be an important predictor of lead-induced TR. Hypothetically speaking, if earlier 3-dimensional echocardiography had been performed in our reported case, the progression of TR might have been predicted.

In this case, the mechanism of regurgitation was elucidated by three-dimensional echocardiography 9 years after pacemaker implantation, and surgical repair was straightforward.

**Conflict of interest** None.

## References

1. Lin G, Nishimura RA, Connolly HM, et al. Severe symptomatic tricuspid valve regurgitation due to permanent pacemaker or implantable cardioverter-defibrillator leads. *J Am Coll Cardiol.* 2005;45:1672–5.
2. Seo Y, Ishizu T, Nakajima H, et al. Clinical utility of 3-dimensional echocardiography in the evaluation of tricuspid regurgitation caused by pacemaker leads. *Circ J.* 2008;72:1465–70.

特集：左心低形成症候群に対する治療戦略

## Norwood 手術における Blalock-Taussig シェント — 実験から臨床への展開 —

北 市 隆  
黒 部 裕 嗣

菅 野 幹 雄  
神 原 保

木 下 肇  
藤 本 鋭 貴

中 山 泰 介  
北 川 哲 也

〔胸部外科〕 第 67 卷 第 4 号〔2014 年 4 月号〕 別刷

— 南 江 堂 —



# Norwood 手術における Blalock-Taussig シヤント — 実験から臨床への展開

北 市 隆  
黒 部 裕 嗣

菅 野 幹 雄  
神 原 保

木 下 肇  
藤 本 鋭 貴

中 山 泰 介  
北 川 哲 也\*

## はじめに

Norwood 手術における肺血流路再建法において右室-肺動脈 (RV-PA) シヤントは、早期生存率を画的に改善させたが<sup>1,2)</sup>、一方では中期遠隔期における右室切開に伴う右室機能低下や不整脈などの発生などの問題点も指摘されることから<sup>3,4)</sup>、Blalock-Taussig (BT) シヤントを第一選択とする、あるいはそれに回帰する施設も多く、その選択にはいまだ論議のあるところである。

一方、Norwood 手術における BT シヤントによる肺血流のコントロールは周術期管理により改善されたが、もっとも重要な点はシヤントサイズと考えられ、小さめの人工血管使用が唱えられてきた。

今回、われわれが行ってきた Norwood 手術における肺血流がコントロール可能な BT シヤントのサイズの実験的検討<sup>5,6)</sup>と実際の臨床について述べる。

## I. 実験的検討

われわれは Norwood 循環特性を解明し、至適な体肺動脈シヤントのガイドラインを確立するために一連の研究を行ってきた。

まず、乳児期早期に肺血流を動脈管に依存する肺動脈閉鎖に伴う疾患群において、実際の体肺動脈シヤント術の短絡肺血流量を測定し、至適な短絡肺血流量が 70~90 ml/kg/分であることを明ら

かにした。次に、ローラーポンプと塩化ビニール管で作成した Norwood 手術後の剛性並列循環モデルを作成し、血液で充填して任意に肺血管抵抗を変動させ、200~300 ml/分の肺血流量を得るための体肺動脈シヤント法について検討した。その結果から、実際の乳児期早期例での Norwood 手術の腕頭動脈からのシヤントを想定すると、3.0~3.5 mm 径の人工血管による体肺動脈シヤントが望ましいと考えた<sup>5)</sup>。

さらに生体の有する心機能の変化、血管の弾性などを考慮し、イヌ単心室 Norwood 循環モデルを用いて、鎖骨下動脈-肺動脈シヤントのサイズと  $Paco_2$ 、 $Fio_2$ 、ヘマトクリットなどの生理的因子が Norwood 循環特性に及ぼす影響について明らかにし、Norwood 手術の BT シヤントのサイズに関する有用な指標の作成を試みた。すなわちある一定の大きさを越えたシヤントでは、もはや呼吸調節による  $Paco_2$ 、 $Fio_2$  などの変化や薬物投与による血管抵抗の変化などでは影響が及ばない肺血流過多の状態に陥ると考えた。

Mora らが報告した単心室モデル<sup>7)</sup>に準じたイヌ単心室 Norwood 循環モデルを作製し、呼吸器設定 ( $Fio_2$ 、呼吸数、気道内圧) を変化させたときの体血圧、肺動脈圧、中心静脈圧、左房圧およびその際の肺血流量 ( $Qp$ )、体血流量 ( $Qs$ ) を測定した。シヤントサイズの影響を評価するために、シヤントサイズ (mm)/体重 (kg) [SS/BW] 別に、 $Qp$  の規制因子とされる  $Paco_2$ 、 $Fio_2$ 、へ

キーワード：Norwood 手術、体肺動脈短絡術、シヤントサイズ、イヌ単心室モデル

\*T. Kitaichi (准教授)、M. Sugano、H. Kinoshita、T. Nakayama、H. Kurobe、T. Kanbara、E. Fujimoto、T. Kitagawa (教授)：徳島大学心臓血管外科。

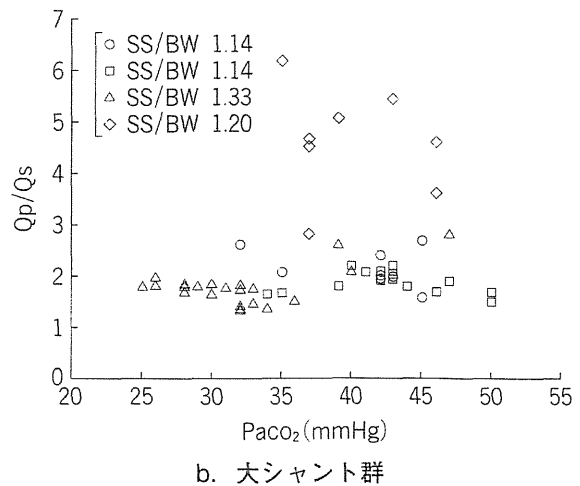
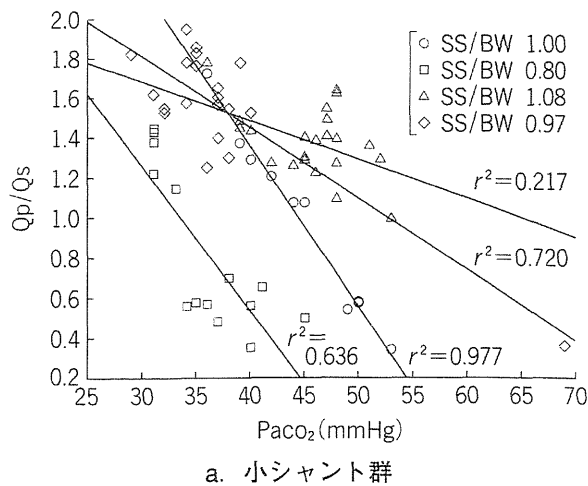


図 1. Qp/Qs-Paco<sub>2</sub> (文献6より引用)

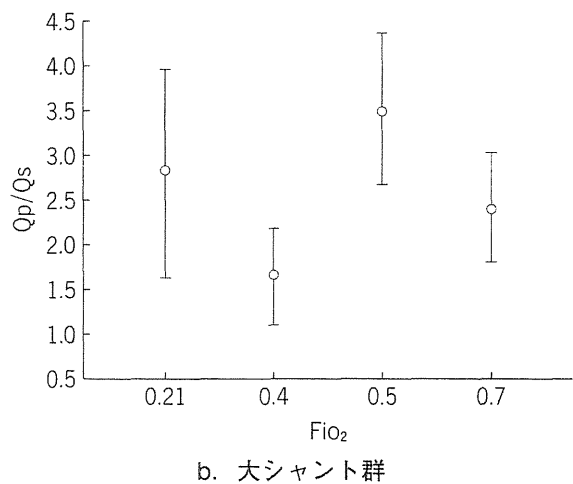
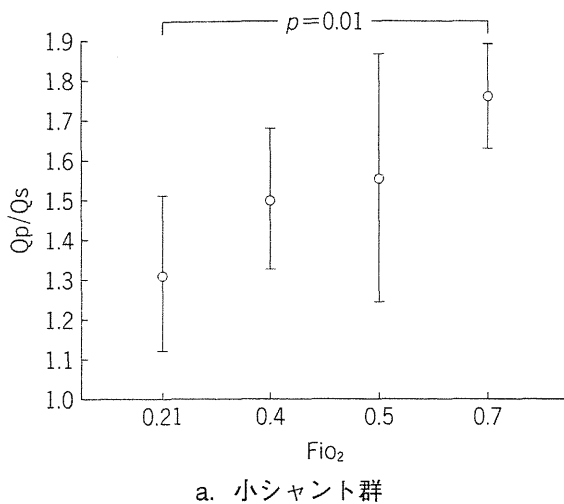


図 2. Qp/Qs-Fio<sub>2</sub> (文献6より引用)

マトクリット、base excess と Qp/Qs. Qs の関係について解析した. SS/BW は 0.80~1.33 (平均  $1.08 \pm 0.16$ ) に分布し、0.8~1.1 を小シャント (S) 群 ( $n=4$ ), 1.1~1.4 を大シャント (L) 群 ( $n=4$ ) とした. この結果、以下の5点が明らかとなった.

1) Qp/Qs と Paco<sub>2</sub> の関係は、S 群で有意な負の相関関係を認められたが、L 群では相関関係を認めなかった (図 1).

2) Qs と Paco<sub>2</sub> の関係では、S 群では Qs も至適値で推移し、SS/BW が小さいほど Paco<sub>2</sub> の変化に対し Qs の変化率が大きかった. 一方、L 群では Qs と Paco<sub>2</sub> の間に相関を認めなかった.

3) Qp/Qs と Fio<sub>2</sub> の関係は、S 群では Fio<sub>2</sub> が高くなると Qp/Qs は有意に増大した. 一方、L

群では相関を認めなかった (図 2).

4) ヘマトクリット値の変化は、両群ともに Qp/Qs に有意な影響を与えなかった.

5) Qp/Qs と base excess の関係は、両群ともに有意な相関を認めなかったが、S 群では Qp/Qs と base excess の分布が血行動態的に許容域にあったが、L 群では心肺虚脱と重度のアシドーシス域にあった.

以上から、SS/BW が 0.8~1.1 のとき、Qp/Qs が Paco<sub>2</sub> や Fio<sub>2</sub> 変化などの呼吸性の調節で規制できるのに対し、それよりも大きなシャントでは肺血流量過多になり、規制不可能な心肺虚脱状態になった. したがって適切な Qp, Qs を得るには、SS/BW 0.9~1.0 が Norwood 手術時の至適

な体肺動脈シャントサイズとして妥当ではないかと考えた<sup>6)</sup>。

## II. 臨床的経緯

1993~2000年にかけて行われたBTシャントを用いたNorwood手術では、体重2.6~3.5kgの症例に対し3.5~4.0mmのシャントが用いられたが、SS/BW>1.1ではすべて高肺血流にて死亡している。この経験から先述の実験的検討をすすめる一方、RV-PAシャントの良好な成績が報告されたことから、2002~2010年代はRV-PAシャントを主として用いてきた。体重3kg未満では4mm、3kg以上で5mmのRV-PAシャントを用いたが、それでもクリッピングなどで肺血流の規制を必要とすることも多く、逆に予期せぬRV-PAシャント狭窄や閉塞を経験した経緯やRV切開の手技の煩雑さも考慮し、2010年以降、体重3.0kg以上、大動脈弁狭窄で上行大動脈径が3mm以上あるような症例を選んでBTシャントを選択するようになった。最近われわれが経験したBTシャントによるNorwood手術において、シャントサイズに一考を要した症例を提示する。

**症例** 在胎38週3日、男、3,602gで出生、左心低形成症候群。

大動脈弁閉鎖、僧帽弁閉鎖であり、上行大動脈内径は術前CT上約3.0mmであった。日齢11日にNorwood手術を行った。上行大動脈の外径は5mmと比較的太く、体重も3.5kgを超えていたことから肺血流路再建はBTシャントを選択した。術後の肺血流過多を懸念し、右腕頭動脈から右肺動脈との間に3.0mm ePTFE グラフトによるBTシャントを作製した。人工心肺離脱後、 $\text{Fio}_2$  1.0、NOガス吸入にて $\text{Spo}_2$  60~70%、 $\text{Po}_2$  30mmHg前後で経過したが、集中治療室(ICU)帰室後から低肺血流が原因と思われる $\text{CO}_2$ 貯留がコントロールできず、シャントのサイズアップを余儀なくされた。同日、BTシャントを3.0mmから3.5mmへ変更、高炭酸ガス血症は改善し、以後安定した血行動態を示した。現在Glenn手術が完了し、Fontan手術の待機中である。

## III. 考 察

Norwood手術における肺血流路再建法におい

てRV-PAシャントは、早期生存率を画期的に改善させたが<sup>1,2)</sup>、一方では中期遠隔期における右室切開に伴う右室機能低下や不整脈、右室切開部の瘤形成やRV-PAシャントや近接する肺動脈の高度狭窄などの問題点の報告<sup>3,4,8)</sup>もあり、BTシャントを第一選択あるいはそれに回帰する施設も存在する。2010年に報告されたNorwood手術における肺血流路に関する臨床試験では、12ヵ月時における移植を回避した生存率はRV-PAシャント群のほうがBTシャント群より良好であったが、シャントや肺動脈に対する意図せぬインターベンションの介入はRV-PAシャントのほうが有意に高率であり、さらに12ヵ月以降は生存率や右室機能に両群間で有意差は認められず、両者の優位性はさらなる検討を要すると結論づけられている<sup>9)</sup>。

BTシャントによる肺血流のコントロールは、low resistance strategyなどの周術期管理により改善されたが<sup>10)</sup>、もっとも重要な点はシャントサイズと考えられ、古くから小さめの人工血管使用が唱えられてきた。今回報告した実験は、まだRV-PAシャントや現在のような周術期管理が確立される以前にNorwood術後の肺血流規制に難渋していた際に計画されたものであるが、現在においてもシャントサイズの選択は非常に重要な因子であると考えられる。

先述の症例においてイヌ単心室モデルにて得られた指標に照らし合わせると、3.0mmのシャントはSS/BW 0.83、3.5mmでは0.97となる。したがって3.0mmのシャントは境界下限になり、人工心肺時間や肺血管床の環境によっては低肺血流となる可能性を秘め、一方3.5mmでは高肺血流の可能性を指摘されるかもしれない。実際の臨床では、使用可能な人工血管は3.0mm、3.5mm、4.0mmと限られているため、どのサイズを選択してもSS/BW 0.9~1.0のボーダーラインになることも多い。このためSS/BW 0.9~1.0を一つの基準とし、患者因子(手術時日齢、解剖学的要素、術前状態など)や術式によってサイズを決定する必要があると考えている。

## おわりに

1) イヌ単心室Norwood循環モデルのBTシャントにおいて、SS/BW 0.9~1.0を満たすシャン

トでは生理的な呼吸調節にて肺血流量をコントロール可能であった。

2) この指標は患者因子などを考慮する必要はあるが、ヒトにおける Norwood 手術においても有用であると考ええる。

## 文 献

- 1) Sano S, Ishino K, Kawada M et al : Right ventricle-pulmonary artery shunt in first-stage palliation of hypoplastic left heart syndrome. *J Thorac Cardiovasc Surg* **126** : 504-509. 2003
- 2) Barron DJ : The Norwood procedure : in favor of the RV-PA conduit. *Semin Thorac Cardiovasc Surg Pediatr Card Surg Annu* **16** : 52-58. 2013
- 3) Tanoue Y, Kado H, Shiokawa Y et al : Mid-term ventricular performance after Norwood procedure with right ventricular-pulmonary artery conduit. *Ann Thorac Surg* **78** : 1965-1971. 2004
- 4) Alsoufi B, Bennetts J, Verma S et al : New developments in the treatment of hypoplastic left heart syndrome. *Pediatrics* **119** : 109-117. 2007
- 5) Kitagawa T, Katoh I, Fukumura Y et al : Achieving optimal pulmonary blood flow in the first-stage of palliation in early infancy for complex cardiac defects with hypoplastic left ventricles. *Cardiol Young* **5** : 21-27. 1995
- 6) Kitaichi T, Chikugo F, Kawahito T et al : Suitable shunt size for regulation of pulmonary blood flow in a canine model of univentricular parallel circulations. *J Thorac Cardiovasc Surg* **125** : 71-78. 2003
- 7) Mora GA, Pizarro C, Jacobs ML et al : Experimental model of single ventricle : influence of carbon dioxide on pulmonary vascular dynamics. *Circulation* **90** [5 Pt 2] : II-43-II-46. 1994
- 8) Rumball EM, McGuirk SP, Stümper O et al : The RV-PA conduit stimulates better growth of the pulmonary arteries in hypoplastic left heart syndrome. *Eur J Cardiothorac Surg* **27** : 801-806. 2005
- 9) Ohye RG, Sleeper LA, Mahony L et al : Comparison of shunt types in the Norwood procedure for single-ventricle lesions. *N Engl J Med* **362** : 1980-1992. 2010
- 10) Nakano T, Kado H, Shiokawa Y et al : The low resistance strategy for the perioperative management of the Norwood procedure. *Ann Thorac Surg* **77** : 908-912. 2004

## SUMMARY

### Reconstruction of Pulmonary Blood Flow in the Norwood Procedure : Blalock-Taussig shunt : from Bench to Surgery

*Takashi Kitaichi, Department of Cardiovascular Surgery, The University of Tokushima, Tokushima, Japan*

*Mikio Sugano, Hajime Kinoshita, Taisuke Nakayama, Hirotsugu Kurobe, Tamotsu Kanbara, Eiki Fujimoto, Tetsuya Kitagawa*

Although the right-ventricle to pulmonary artery (RV-PA) shunt as a source of pulmonary blood supply of Norwood procedure has improved early outcomes, disadvantages including right ventricular dysfunction or arrhythmias have been reported. So it has been still remained controversial whether BT shunt or RV-PA conduit should be selected. We examined the influence of Blalock-Taussig (BT) shunt size on regulation of the pulmonary blood flow in experimental model of a univentricular heart to determine the specific guidelines regarding suitable shunt size in the Norwood procedure.

The canine univentricular heart model with the ratio of shunt size to body weight (SS/BW) of 0.8 to 1.1 showed significant negative correlation between the pulmonary/systemic blood flow ratio (Qp/Qs) and arterial PCO<sub>2</sub>, but those with SS/BW of 1.1 to 1.4 did not. Similar phenomena were shown with the grouped data on relationship between the Qp/Qs and inspired oxygen fraction. These findings imply that when SS/BW is 0.8 to 1.1, the Qp/Qs is controllable by physiologic respiratory manipulations.

In the context of our clinical experiences, SS/BW of 0.9 to 1.0 is considered a useful index for suitable BT shunt in the Norwood procedure.

## KEY WORDS

Norwood procedure/Blalock-Taussig shunt/shunt size/canine univentricular heart model